LOOP MODELING OF X-RAY CORONAE: SOLAR-TYPE STARS IN YOUNG CLUSTERS AND ASSOCIATIONS

A. MAGGIO, G. MICELA, G. PERES
Istituto e Osservatorio Astronomico "G.S. Vaiana", Palermo, Italy

ABSTRACT. The disk-integrated X-ray emission from late-type stars originates from hot coronal plasmas most likely confined in closed magnetic structures, of the kind clearly observed on the Sun. The complex plasma temperature stratification in such structures can be described accurately using hydrostatic coronal loop models, which can be adopted to synthesize the X-ray emission, and to fit the observed X-ray spectra. The spectral analysis with loop models allows us to get physical insight into the properties of stellar coronae, including indications on the loop geometry and on the plasma heating, and hence to study how the coronal structures may change with the ageing of the stellar magnetic activity. In this context, we present preliminary results from the analysis of ROSAT/PSPC spectra of selected G-type stars in young open clusters and associations.

1. Introduction

The rationale for coronal loop modeling is given essentially by the solar-stellar analogy. Spatially-resolved X-ray images of the solar corona show unambiguously that the totality of the X-ray emission originates from hot plasma magnetically-confined in loop-like structures, often crowded in groups. There are several indications that the X-ray emission from late-type stars shares a similar origin, but the lack of sufficient spatial resolution prevents us from studying *directly* the geometrical and thermodynamical properties of stellar coronal structures. For this reason, in order to get such an information, we may resort to the available spectral data.

The physical insight we would like to get here is how the characteristics of stellar coronal structures change vs. X-ray activity level, and the consequent implications on the local plasma heating, magnetic fields, and the related magnetic dynamo mechanism, in different phases of stellar evolution.

To this aim, our approach is to perform spectral fitting of the observed stellar X-ray emission with detailed coronal loop models. In the following, we present preliminary results of an application of this loop modeling approach to ROSAT/PSPC X-ray spectra of 7 selected G-K type stars in young clusters and associations.

2. The method

In order to compute the plasma temperature and density distributions vs. field line coordinate we adopt the hydrostatic coronal loop model of Serio et al. (1981), with the enhancements described in Ciaravella et al. (1996), to which we refer for further details.

Here it is useful to recall that, assuming uniform heating throughout the loop volume, the model is entirely described by two parameters, selected among the following: plasma maximum temperature at loop top, $T_{\rm max}$, plasma pressure at loop base, p_0, loop semi-length, L, and heating per unit volume, $E_{\rm H}$. In particular, these quantities are linked together by the scaling laws:

$$T_{\rm max} \simeq 1.4 \times 10^3 \ (p_0 L)^{1/3} \exp(0.04 \ L/s_p) \ \ {\rm K} \tag{1}$$

$$E_{\rm H} \simeq 10^5 \ p_0^{7/6} L^{-5/6} \ \exp(-0.5 \ L/s_p) \ \ {\rm erg \ cm^{-3} \ s^{-1}} \tag{2}$$

where $s_p \simeq 5 \times 10^3 T_{\rm max} \ g_*/g_\odot$ is the pressure scale height, evaluated at the loop apex.

Given the plasma temperature and density distributions within the loop, the volume-integrated, optically-thin, X-ray spectrum can be easily synthesized and convolved with the instrument energy response, in order to produce a photon X-ray spectrum which can be directly compared with the observation.

The spectral fitting proceeds as follows. We first compute a set of loop model spectra for different values of the *two free parameters*, $T_{\rm max}$ and L. The motivation and advantages of this choice are described in Maggio & Peres 1997. Then we search for the best-fit model which yields the minimum χ^2 value, in the assumption that the X-ray emission comes almost entirely from one class of coronal loops all with the same characteristics (1-loop modeling). At the same time we get a normalization factor, and more specifically the surface filling factor, f, i.e. the fraction of the stellar surface covered by loop footpoints. If the 1-loop fitting does not yield an acceptable χ^2, or if the best-fit model is physically unrealistic (see examples below), then we perform a two-loop model fitting, in which two dominating classes of coronal loops are assumed to contribute to the observed X-ray spectrum. If a successful fit is obtained, we compute statistical confidence regions in the (1-loop or 2-loop) model parameter space, following the prescription of Lampton et al. (1976), based on the $\Delta\chi^2$ statistics. Note that the visualization and interpretation of the confidence regions in the 2-loop model parameter space is complicated by the high dimensionality of such space, but it can be achieved as described in Maggio & Peres (1997), and shown in the application presented below.

The diagnostic power of our loop model fitting approach has been extensively studied through self-consistent simulations (Maggio & Peres 1996). As expected, we have found that it depends on the observing instrument (i.e. on the available spectral resolution and energy band) and on the photon counting statistics, but also on the intrinsic loop characteristics. In fact, for loops with $L \ll s_{\rm p}$, i.e. shorter than the pressure scale height, $T_{\rm max}$ can be constrained, and hence the product $p_0 L$ (see Eq. 1), but not *independently* L or p_0, because of a scale invariance of the equations governing the loop model (Maggio & Peres 1996). Since

$$f \ \propto \ L \, T_{\rm max}^{-7/2} \ F_{\rm X} \tag{3}$$

also the filling factor cannot be constrained; on the other hand, the physical condition $f \leq 1$ may be used to put an upper limit on L and a lower limit on p_0.

Instead, for loops with $L \sim s_{\rm p}$ or longer, all loop parameters could be constrained, given spectra with high signal-to-noise ratio (Maggio & Peres 1996).

Other approaches have been used in the past to infer the properties of stellar coronal structures. One of such approaches is to fit the X-ray spectra with simple models, e.g. 2-component isothermal (2-T) models or models assuming a power-law emission measure (PLEM) distribution, and then interpret the fitted temperatures and X-ray luminosities (L_X) as due to loop structures, using the loop scaling laws (Giampapa et al. 1996; Preibisch 1997). There are caveats and pitfalls to consider, however: first, a successful 2-T model does not warrant necessarily a 2-loops description, because 1-loop spectra can be (sometimes) satisfactorily fitted with 2-T models, as proved by the simulations presented by Ciaravella et al. (1997); moreover, the temperatures derived from isothermal models are strictly lower than T_{max} in coronal loop models, because the former are average values weighted by the emission measure distribution, the plasma emissivity and the instrument response; if a PLEM model is assumed, the best-fit slope of the emission measure distribution is not necessarily in agreement with slopes predicted by loop models; finally, the measured L_X is usually evaluated *in the instrument energy band*, and it cannot be equated to the loop total heating, $E_H\ V$, as often assumed.

3. The application

3.1. Star sample

In the present context, we have analyzed the X-ray coronal emission of solar-type stars in young clusters and associations, with the aim to investigate – with the help of the insight coming from loop modeling – how the coronal structures change with time. In fact, the X-ray emission level of G-type stars decreases by a factor $\sim\ 10^4$ for increasing stellar ages from the WTTS phase ($\sim\ 5 \times 10^6$ yr) to the age of the Sun ($\sim\ 5 \times 10^9$ yr), and there is also evidence of decreasing coronal (mean) temperature by a factor $\sim$ 10. It is not obvious how stellar coronae achieve such changes.

Tab. 1 - Selected stars

Name	Distance (pc)	Spectral Type	$v\ \sin i$ km/sec	Age (yr)	Group
HD 283572	140	G8 IV-V	80	3.5×10^6	WTTS in Taurus
Ced 110	140	K6	75	4×10^6	WTTS in Chameleon I
Hz 253	115	G1 V	40	8×10^7	Pleiades
Hz 739	115	G0 V	13	8×10^7	Pleiades
VB 50	45	G1 V	7	6×10^8	Hyades
VB 64	45	G6 V	5	6×10^8	Hyades
VB 77	45	F7 V	25	6×10^8	Hyades

We have selected seven G-K type stars observed with ROSAT/PSPC, in order to perform loop model fitting of their X-ray spectra. Two of them (HD 283572 and Ced 110) are classified as Weak T Tauri Stars (WTTS), belonging to the Taurus and Chameleon I associations, respectively; the others are members of the Pleiades (Hz 253, Hz 739) and the Hyades (VB50, VB64, VB 77) open clusters. Some properties of such stars are reported in Tab. 1. Note that since we require high signal-to-noise X-ray spectra for

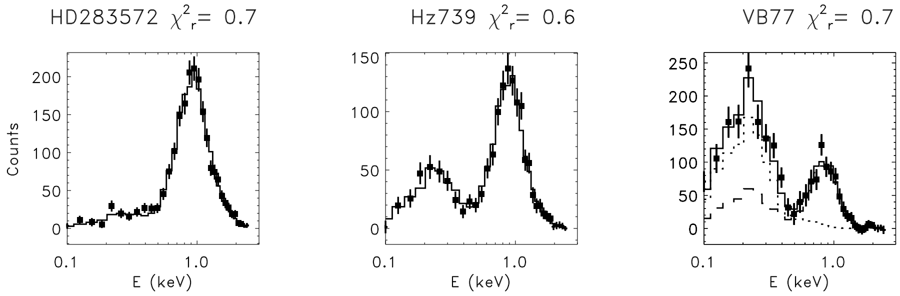

Fig. 1. ROSAT/PSPC X-ray spectra of HD 283572 (WTTS) and Hz 739 (Pleiades), with best-fit 1-loop model spectra, and of VB 77 (Hyades) with with best-fit 2-loop model spectra. In the latter case the contributions to the total spectrum due to the individual loop components are also shown (dashed and dotted lines).

our analysis, these stars are among the most luminous of their class in each cluster or association.

3.2. Results

We have obtained successful 1-loop model fitting for the selected Pleiades and WTTS. In Fig. 1 we show the spectra of one WTTS (HD 283572) and one of the Pleiades members (Hz 739), together with the best-fit 1-loop model spectra, and the spectrum of one of the Hyades members (VB 77), whose 2-loop model fitting is discussed in the following. In Fig. 2 we show instead an example of the 90% confidence regions in the 1-loop model parameter space, which we have computed for each star. The figure shows that $T_{\rm max}$ is well constrained in the range 1.3 – 2.7 $\times 10^7$ K, while L is bounded to be less than the pressure scale height, $s_{\rm p} \simeq 10^{11} T_7$ cm, by the 90% confidence contour, and the base pressure must be larger than $\simeq$ 30 dyn cm^{-2}. As explained above, in such a case (loops shorter than the pressure scale height) L and p_0 cannot be determined independently: the same X-ray luminosity (or surface flux) can be achieved either with very short loops with high pressure, covering a small fraction of the stellar surface, or with relatively longer, low-pressure loops, and larger filling factors.

For the Hyades stars, 1-loop models fail to yield acceptable χ^2 values, and 2-loop models are required to fit the observed X-ray spectra. Even more relevant than the best-fit models are the confidence regions in the 2-loop parameter space, because they give you the acceptable parameter ranges. Two cross-sections of a typical 4-dimensional confidence region are shown in Fig. 3: these 2-D sections are slices in the $T_{\rm max} - L$ plane of each loop component, obtained by fixing the other loop component at the best-fit position. In the same figure, the loci where the entire stellar surface is covered by loop structures (total filling factor $f = f_1 + f_2 = 1$) are drawn. For more details on the way to explore and interpret the whole 2-loop model parameter space we refer to Maggio & Peres (1997). In the present example, we have found that $T_{1\rm max}$ is well constrained in the range 1.2 – 3.2 $\times 10^6$ K, while the semi-length of the cooler loop is bounded by the

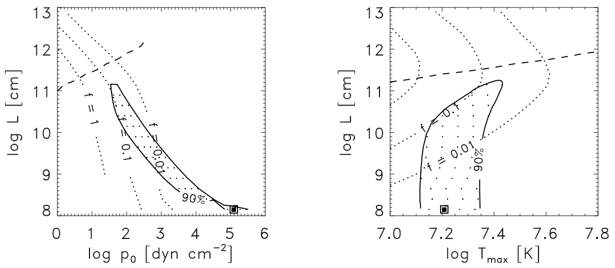

Fig. 2. Statistical confidence regions (solid lines), at the 90% confidence level, drawn in the L-p_0 plane (left panel), and in the L-$T_{\rm max}$ plane, for the 1-loop modeling of Hz 739. The dashed lines indicate the locus where the loop height is equal to the pressure scale height, $s_{\rm p}$. The dotted lines are contour levels at three values of the surface filling factor, $f = 0.01, 0.1, 1$. The square marks the best-fit 1-loop model.

$f < 1$ constraint to be $L_1 < 8 \times 10^8$ cm. Instead, only a lower limit on the maximum temperature of the hotter loop, $T_{2\rm max} > 6 \times 10^6$ K, is determined by the 90% confidence region. There is no other constraint imposed on the hot-loop component, either by the confidence region or by the requirement $f < 1$. In such a case, since loops much larger than the stellar radius are not physically realistic, we usually restrict our attention to solutions where also the high-$T_{\rm max}$ loops are shorter than the pressure scale height. We stress that, with the present data available, this choice is only motivated by obtaining physically plausible 2-loop model solution, and by the analogy with the solar corona, where the hotter plasma tends to be confined in the more compact structures. This choice allows in most cases to put also an upper limit on $T_{2\rm max}$ and on f, as well as a lower limit on the base pressure of the hot loops.

Tab. 2 - Summary of results

	WTTS	Pleiades	Hyades	
Parameter	1-loop best-fit		2-loop best-fit	
			low-$T_{\rm max}$ loops	high-$T_{\rm max}$ loops
$T_{\rm max}$ (K)	$1.3 - 3.6 \times 10^7$		$1 - 6 \times 10^6$	$6 - 30 \times 10^6$
L (cm)	$< 10^{11} \simeq s_p$ (a)		$10^8 - 10^9$	unconstrained
p_0 (dyn cm^{-2})	$> 10 - 100$		$> 2 - 10$	$> 5 - 40$ (b)
f	$< 0.1 - 1$		< 1	$< 0.05 - 0.5$ (b)
$L_{\rm X}$ (erg s^{-1}) (c)	1.6×10^{31}	$1 - 3 \times 10^{30}$	$0.36 - 2.8 \times 10^{29}$	$0.95 - 4.4 \times 10^{29}$

(a) 90% confidence region constraint.

(b) Assuming $L_{\rm hot} < s_p$.

(c) In the 0.1 – 2.4 keV band.

The results of the 1-loop and 2-loop fitting of the selected X-ray spectra are summa-

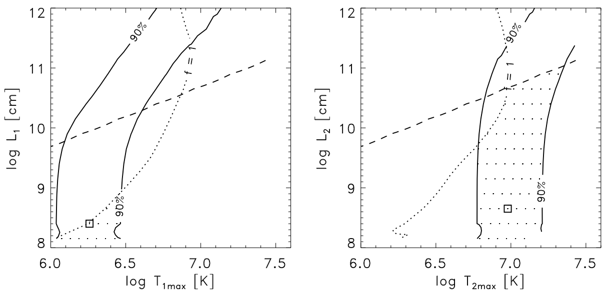

Fig. 3. Confidence regions at the 90% level in the $T_{1\max} - L_1$ plane, for each component of the 2-loop model analysis of VB 77, obtained by fixing the other loop component at the best-fit location (square symbols). The allowed region where the total fitting factor $f = f_1 + f_2 < 1$ is shaded. The loci where the loop height equals the pressure scale height, $s_{\rm p}$, are indicated by the dashed lines.

rized in Tab. 2, where we report the ranges of model parameters found with our analysis for the three stellar groups, together with the computed X-ray luminosities. Note that, in the case of the Hyades stars, the separate contributions of the low-$T_{\max}$ loops and of the high-$T_{\max}$ loops are indicated.

Finally, in Fig. 4 we show plots of the surface X-ray flux vs. $T_{\max}$ and vs. p_0, for the stars in our sample, and two points indicating nominal values of the quiet and active solar corona (Mewe 1991), for ease of comparison. Note that the 1-loop best-fit models for the WTTS and for the Pleiades stars are indicated with one symbol for each star, while two symbols are plotted for each of the Hyades stars, in order to show the 2-loop components separately.

4. Conclusions

The ROSAT/PSPC X-ray spectra of the solar-type young stars in our sample can be successfully described with coronal loop models. In the present application, firm constraints can be derived for $T_{\max}$ in all cases. High-T loop components ($T_{\max} \simeq 0.6 - 4 \times 10^7$ K) have been found for all selected stars, while indication of low-T loops ($T_{\max} \simeq 1 - 6 \times 10^6$ K) has been found only for the Hyades sources.

The available spectra allow to put lower limits on p_0, provided in some case by the physical constraint on the total surface filling factor, $f < 1$, or in other cases by the assumption that the loops are smaller than the pressure scale height ($L < s_p$). In any case, due to the scale invariance of the model equations, filling factors (and loop lengths) are poorly constrained; however, for any given component at $T_{\max}$, the following relation holds:

$$f \simeq 0.52 \left(\frac{R_*}{R_\odot}\right)^{-2} \left(\frac{L}{10^{10}}\right) \left(\frac{T_{\max}}{10^7}\right)^{-7/2} \alpha \, \frac{L_{\rm X}}{10^{30}} \qquad (4)$$

where α is the fraction of the total energy input which goes into radiative emission *in the X-ray band considered*; moreover, the volumetric heating, in each loop, obeys the

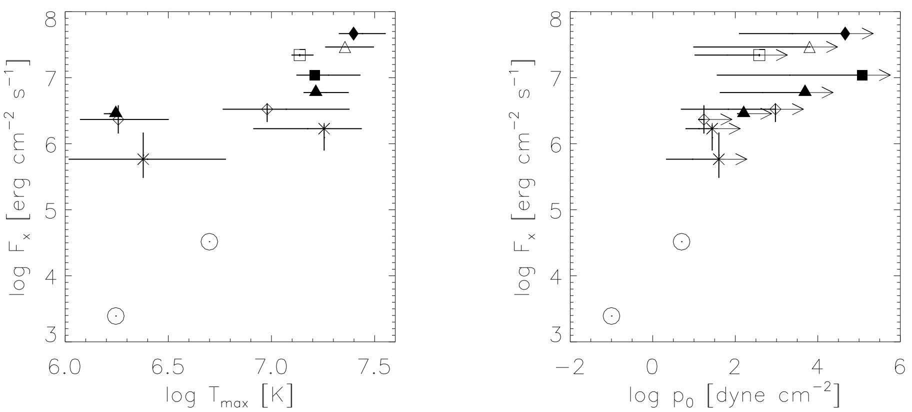

Fig. 4. X-ray surface fluxes vs. $T_{\max}$ and vs. p_0, for each loop component of the 1-loop and 2-loop model fitting of the sample X-ray spectra. The symbols (empty triangle for HD 283572, square for Ced 110, filled diamond for Hz 253, filled square for Hz 739, filled triangle for VB50, asterisk for VB 64, diamond for VB77) indicate the best-fit solutions, and the vertical and horizontal bars the parameter ranges spanned by the 90% confidence regions. The open circles mark the indicative quiet and active Sun flux (Mewe 1991)

following scaling law:

$$E_{\rm H} \simeq 0.03 \left(\frac{T_{\max}}{10^7}\right)^{7/2} \left(\frac{L}{10^{10}}\right)^{-2} \text{ erg cm}^{-3} \text{ s}^{-1} \tag{5}$$

so that very short loop solutions imply small filling factors, very high heating rates, and very high plasma pressures

$$p_0 \simeq 36.4 \left(\frac{L}{10^{10}}\right)^{-1} \left(\frac{T_{\max}}{10^7}\right)^{3} \text{ dyn cm}^{-2} \tag{6}$$

We find that the low-T loops in the Hyades G stars have $T_{\max}$ similar to the large scale structures (LSS) in the quiet solar corona, while the high-T loops, present in all the stars we have studied, are substantially hotter than solar active regions. On the other hand, the plasma pressures are very high in all cases; in particular, also the low-T loops in the Hyades appear to have pressures at least two orders of magnitude larger than the LSS on the Sun, because our analysis indicates that these loops are relatively short (see Tab. 2), while the loops in the solar LSS reach heights comparable to the pressure scale height; since the $T_{\max}$ values are similar, the loop model scaling law (see Eq. 1) indicates that the plasma pressure must be higher where the loop lengths are shorter. The low-T loops contribute 30% – 70% of the total $L_{\rm X}$ of the Hyades coronae, which are the least X-ray luminous in our sample. The Pleiades and the WTTS have $L_{\rm X}$ larger by one and two orders of magnitude, respectively, as expected on the basis of the activity-age relationship for late-type stars (see for example Damiani et al. 1995).

We conclude by stressing that loop models sometimes work very well, and in other cases they provide only upper or lower limits on the relevant physical quantities, but the coronal loop parameters are always uniquely tied together by well tested scaling laws, so that loop modeling eventually provides a better physical insight on stellar coronae than achievable with simpler models.

In order to constrain better the characteristics of stellar coronae, loop modeling may be usefully complemented by variability studies, flaring loop modeling, emission measure analyses and line density diagnostics (provided by high resolution spectra, as those available, e.g., with EUVE). Looking to the future, we recognize that an important challenge for coronal loop modeling will be their application to the analysis of the high-resolution X-ray spectra that will be soon obtained with the new space observatories AXAF and XMM.

Acknowledgements

We acknowledge the stimulus to pursue this research activity provided by Prof. S. Serio, as well as by the many colleagues interested to the field of X-ray activity in late-type stars.

References

Ciaravella, A., Peres, G., Maggio, A., Serio, S.: 1996, *Astron. Astrophys.* **306**, 553.

Ciaravella, A., Maggio, A., Peres, G.: 1997, *Astron. Astrophys.* **320**, 945.

Damiani, F., Micela, G., Sciortino, S., Harnden, F.R., Jr.: 1995, *Astrophys. J.* **446**, 331.

Giampapa, M.S., Rosner, R., Kashyap, V., Fleming, T.A., Schmitt, J.H.M.M., Bookbinder, J.A.: 1996, *Astrophys. J.* **463**, 707.

Lampton, M., Margon, B., Bowyer, S.: 1976, *Astron. Astrophys.* **208**, 177.

Maggio, A., Peres, A.: 1996, *Astron. Astrophys.* **306**, 563.

Maggio, A., Peres, A.: 1997, *Astron. Astrophys.* **325**, 237.

Mewe, R.: 1991, *Adv. Space Res.* **11**, 127.

Preibisch, T.: 1997, *Astron. Astrophys.* **320**, 525.

Serio, S., Peres, G., Vaiana, G.S., Golub, L., Rosner, R.: 1981, *Astrophys. J.* **243**, 288.